

Rare decay searches at the Tevatron

C.-J. Lin^a on behalf of the CDF and DØ Collaborations

^aFermi National Accelerator Laboratory, P.O. Box 500 MS318, Batavia, Illinois, 60510, U.S.A.

We present the current status of the rare B decay searches $B_s^0 \rightarrow \mu^+\mu^-$, $B^0 \rightarrow \mu^+\mu^-$, $B^+ \rightarrow K^+\mu^+\mu^-$, $B^0 \rightarrow K^{*0}\mu^+\mu^-$, and $B_s^0 \rightarrow \phi\mu^+\mu^-$ at the Tevatron.

1. INTRODUCTION

The flavor-changing-neutral-current (FCNC) transitions are highly suppressed in the Standard Model (SM) and can only occur through higher order diagrams. These processes can provide important tests of the SM at the level of radiative corrections where Glashow-Iliopoulos-Maiani (GIM) cancellations are important. Furthermore, in many new physics scenarios, additional loop diagrams involving new particles, such as Supersymmetric (SUSY) particles, can significantly alter the decay rates and kinematics of the FCNC processes. Therefore precision measurements of these rare processes are powerful probes of new physics and are complementary to direct collider searches.

At the Tevatron, we have searched for the FCNC decays of $B_{(s)}^0 \rightarrow \mu^+\mu^-$. The SM expectations [1] for these branching fractions are significantly below the current experimental sensitivity. However, in many SUSY extensions of the SM, the branching fraction could be enhanced by one to three orders of magnitude to a level observable by the Tevatron experiments. An observation of these decays at the Tevatron would be unambiguous evidence for physics beyond the SM. In the absence of an observation, any improvements to the limits can be used to constrain significantly many SUSY models [2–4].

The $B \rightarrow X_s l^+l^-$ transition is another important FCNC process that is accessible at the Tevatron. New physics effects could be seen in the forward-backward asymmetry of the strange meson in the dimuon system and/or in the decay rate [5]. At the Tevatron, we have searched

for the following exclusive decay modes: $B^+ \rightarrow K^+\mu^+\mu^-$, $B^0 \rightarrow K^{*0}\mu^+\mu^-$, and $B_s^0 \rightarrow \phi\mu^+\mu^-$. The former two decay modes have been observed at BaBar [6] and Belle [7]. The latter decay mode $B_s^0 \rightarrow \phi\mu^+\mu^-$ has so far evaded experimental detection.

2. DETECTORS AND DATASETS

The CDF [8] and DØ [9] detectors are general-purpose particle detectors for studying $p\bar{p}$ collisions at a center-of-mass energy of $\sqrt{s} = 1.96$ TeV at the Tevatron. Both detectors have good precision silicon vertex detectors and large muon coverage, which are important for the rare decay searches. Another crucial experimental component is the trigger system. At the Tevatron collision energy, the cross section for the inelastic QCD background is about 1000 times larger than the $b\bar{b}$ production. To suppress the large background, both experiments employ a sophisticated three-tier trigger system to filter collision events and select interesting physics events to store to tape for offline analysis. The data samples for the rare B decay searches are primarily collected using the dimuon triggers. For the results presented here, the sample size used by the analyses ranges from 300 pb^{-1} to 1 fb^{-1} .

3. $B_{(s)}^0 \rightarrow \mu^+\mu^-$ SEARCHES

The CDF and DØ experiments use similar strategy to search for the rare decay of $B_{(s)}^0 \rightarrow \mu^+\mu^-$. The offline analysis begins by selecting two muon candidates of opposite charge which satisfy the online dimuon trigger requirements.

After applying some loose pre-selection requirements (e.g. transverse momentum p_T of the muon and B candidates), the selected sample is still dominated by combinatorial background and partially reconstructed B hadrons.

For the final event selection, CDF uses the following four discriminating variables: dimuon invariant mass $M_{\mu\mu}$, proper decay length $\lambda = c \cdot M_{\mu\mu} L_{3D} / |\vec{p}^{\mu\mu}|$, the 3D opening angle $\Delta\Theta$ between vectors $\vec{p}^{\mu\mu}$ and \vec{L} , and B -candidate track isolation I . The vector $\vec{p}^{\mu\mu}$ is the momentum vector of the B candidate, L_{3D} is the 3D decay length projected on the $\vec{p}^{\mu\mu}$ direction, \vec{L} is the displacement vector from the primary to the dimuon vertex, and the B -candidate track isolation is defined by $I = |\vec{p}_T^{\mu\mu}| / (\sum_i p_T^i + |\vec{p}_T^{\mu\mu}|)$, where the sum is over all tracks with $\sqrt{\Delta\eta^2 + \Delta\phi^2} \leq 1$; $\Delta\phi$ and $\Delta\eta$ are the azimuthal angle and pseudo-rapidity of track i with respect to $\vec{p}^{\mu\mu}$. To enhance signal and background separation CDF constructs a multivariate likelihood ratio based on the latter three input variables: I , $\Delta\Theta$, and λ . We define the likelihood ratio to be

$$L_R = \frac{\prod_i \mathbf{P}_s(x_i)}{\prod_i \mathbf{P}_s(x_i) + \prod_i \mathbf{P}_b(x_i)}, \quad (1)$$

where $x_1 = I$, $x_2 = \Delta\Theta$, $x_3 = \lambda$, and $\mathbf{P}_{s(b)}(x_i)$ is the probability that a signal (background) event has an observed x_i . The probability distributions for the signal events are obtained from the signal Monte Carlo (MC) and the background distributions are taken from the data sidebands. The resulting L_R distributions for the signal and background events are shown in Fig. 1.

In the $D\bar{O}$ analysis background is suppressed by making stringent requirements on the variables $\Delta\Theta$, I , and the transverse decay length significance, $L_{2D}/\sigma(L_{2D})$, where L_{2D} is the projection of \vec{L} onto the plane transverse to the beamline. The L_{2D} -significance is found to have a better discriminating power than L_{2D} alone.

The $B_s^0 \rightarrow \mu^+\mu^-$ branching fraction is obtained by normalizing to the number of $B^+ \rightarrow J/\psi K^+ \rightarrow \mu^+\mu^- K^+$ decays collected by the same trigger. With 780 pb^{-1} (300 pb^{-1}), CDF ($D\bar{O}$) reconstructs about 2400 (900) B^+ candidates. If no signal is observed, the upper limit on the branching fraction can be computed

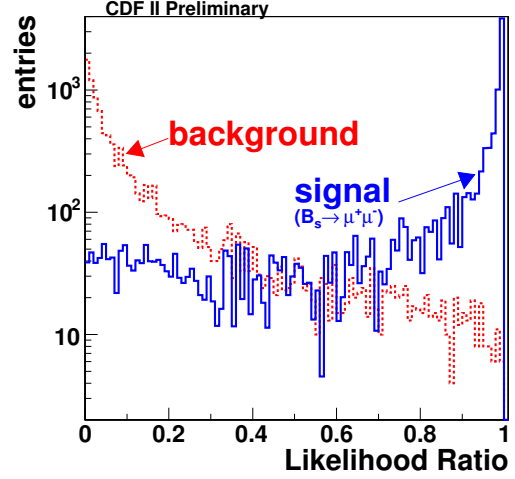


Figure 1. The likelihood ratio distribution for $B_s^0 \rightarrow \mu^+\mu^-$ signal (dashed) from PYTHIA MC and background (solid) from data sidebands.

using the expression

$$\mathcal{B}(B_s^0 \rightarrow \mu^+\mu^-)^{90\%C.L.} = \frac{N_{B_s^0}^{90\%}}{N_{B^+}} \cdot \frac{\epsilon_{B^+}}{\epsilon_{B_s^0}} \cdot \frac{f_u}{f_s} \cdot \mathcal{B}(B^+ \rightarrow J/\psi K^+ \rightarrow \mu^+\mu^- K^+), \quad (2)$$

where $N_{B_s^0}^{90\%}$ is the number of $B_s^0 \rightarrow \mu^+\mu^-$ decays at the 90% C.L. for N observed and N_B expected background events. The value of $N_{B_s^0}^{90\%}$ is estimated using the Bayesian approach assuming a flat prior for the $\mathcal{B}(B_s^0 \rightarrow \mu^+\mu^-)$ and incorporating Gaussian uncertainties into the limit. The parameter $\epsilon_{B_s^0}$ (ϵ_{B^+}) is the total efficiency of the for triggering and reconstructing the signal (normalization) mode. We use the world average fragmentation ratio f_u/f_s and branching fraction $\mathcal{B}(B^+ \rightarrow J/\psi K^+ \rightarrow \mu^+\mu^- K^+)$.

CDF optimizes the analysis based on the *a priori* expected 90% C.L. upper limit on $\mathcal{B}(B_{s,d}^0 \rightarrow \mu^+\mu^-)$. The resulting optimal criteria is $L_R > 0.99$. With the optimized selection requirements and 780 pb^{-1} , there are 1 (2) candidates in the $B_s^0 \rightarrow \mu^+\mu^-$ ($B^0 \rightarrow \mu^+\mu^-$) signal window, as shown in Fig. 2, with an expected background of 1.3 ± 0.4 (2.5 ± 0.4). CDF defines the signal windows as $\pm 70 \text{ MeV}$ about the world aver-

age B_s^0 (B^0) mass, which corresponds to about ± 2.5 times the mass resolution. The expected background is estimated by extrapolating events from the sidebands to the signal region. Given the number of signal events observed is consistent with the background expectation, we computed the following 90% (95%) C.L. limits of $\mathcal{B}(B_s^0 \rightarrow \mu^+\mu^-) < 8.0 \times 10^{-8}$ (1.0×10^{-7}) and $\mathcal{B}(B^0 \rightarrow \mu^+\mu^-) < 2.3 \times 10^{-8}$ (3.0×10^{-8}).

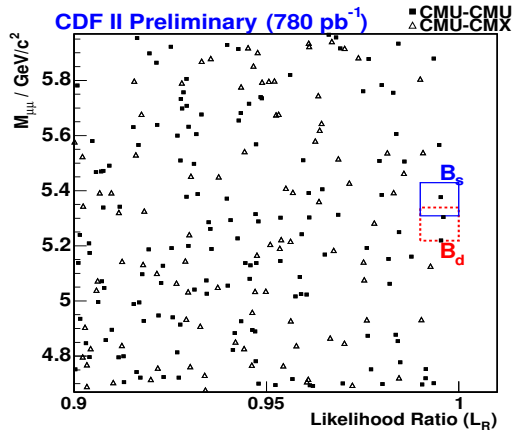


Figure 2. The $\mu^+\mu^-$ invariant mass versus likelihood ratio for central-central (CMU-CMU) and central-forward (CMU-CMX) dimuon trigger samples. The B_s^0 (solid box) and B^0 (dashed box) signal regions are also shown.

DØ optimizes the three discriminating variables using a random-grid search. The optimization resulted in this choice of final selection criteria: $\Delta\Theta < 0.2$ rad, $I > 0.56$, and $L_{2D}/\sigma(L_{2D}) > 18.5$. Based on 300 pb^{-1} of data, there are 4 candidate events in the signal window of $\pm 180 \text{ MeV}$ about the world average B_s^0 mass, as shown in Fig. 3, with an expected background of 4.3 ± 1.2 . The DØ mass resolution is insufficient to discriminate B_s^0 from $B^0 \rightarrow \mu^+\mu^-$ decays. The branching fraction limit is computed assuming the contribution from B^0 is negligible, which is a good approximation for minimal-flavor-violating models. The resulting limit at 90% (95%) C.L. is $\mathcal{B}(B_s^0 \rightarrow \mu^+\mu^-) < 3.2 \times 10^{-7}$ (4.0×10^{-7}). Using the same analysis technique, DØ estimated the

expected 95% C.L. limit with 700 pb^{-1} to be $\mathcal{B}(B_s^0 \rightarrow \mu^+\mu^-) < 2.3 \times 10^{-7}$.

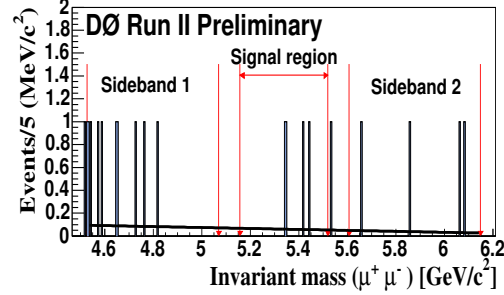


Figure 3. The dimuon mass distribution based on 300 pb^{-1} of DØ data. Four events are observed in the signal region.

4. EXCLUSIVE $B \rightarrow K^{(*)} \mu^+\mu^-$ SEARCHES

In addition to the two-body dimuon decays, the Tevatron has also searched for the $b \rightarrow s \mu^+\mu^-$ FCNC processes. In particular, CDF has searched for the decays of $B^+ \rightarrow K^+ \mu^+\mu^-$, $B^0 \rightarrow K^{*0} \mu^+\mu^-$, and $B_s^0 \rightarrow \phi \mu^+\mu^-$ in 1 fb^{-1} of data. DØ has focused the search in the $B_s^0 \rightarrow \phi \mu^+\mu^-$ channel using 450 pb^{-1} of data.

The offline analysis begins by searching for a pair of oppositely charged muon tracks. The two muon tracks are combined with a third charged track to form a $B^+ \rightarrow K^+ \mu^+\mu^-$ candidate, or another pair of oppositely charged tracks to form a $B^0 \rightarrow K^{*0} \mu^+\mu^-$ or $B_s^0 \rightarrow \phi \mu^+\mu^-$ candidate. The K^{*0} is reconstructed in the mode $K^{*0} \rightarrow K^+ \pi^-$ and the ϕ is reconstructed as $\phi \rightarrow K^+ K^-$. We exclude events where the dimuon invariant mass is within the $J/\psi \rightarrow \mu^+\mu^-$ and $\psi(2S) \rightarrow \mu^+\mu^-$ mass regions to eliminate possible contributions from the charmonium resonant decays.

In the CDF search, muons are required to have $p_T > 1.5$ or 2.0 GeV depending on which dimuon trigger selected the event. The kaon requirement is $p_T > 0.4 \text{ GeV}$. CDF uses the following three discriminating variables in the optimization of the searches. The first variable is the proper decay length significance $\lambda_{2D}/\sigma(\lambda_{2D})$. The λ_{2D} vari-

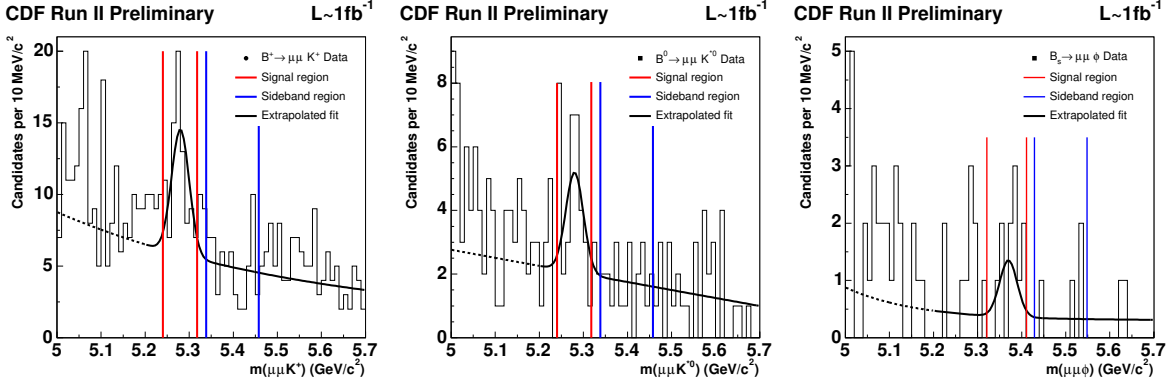


Figure 4. The invariant distribution for the three rare decay modes. The vertical bars define the signal and sideband regions. The black curve illustrates the expected shape for the signal and combinatoric background.

able is defined similarly to the λ variable described earlier, with L_{3D} replaced by the 2D decay length L_{2D} . The second variable is the 2D opening angle $\Delta\alpha$, which is angle between the momentum vector of the B candidate and the decay axis \vec{L} projected onto the transverse plane. The final discriminating variable is the B candidate isolation I . The expected number of background events in the B mass window is obtained by extrapolating events in the high-mass sideband to the signal region. Since the region below the B signal window contains partially reconstructed B decays, only the high-mass sideband is used in the background estimate. The figure-of-merit for the optimization is $S/\sqrt{S+B}$, where S is the estimate of the expected yield of the rare decays, and B is the expected background. For the B^+ and B^0 rare decay searches, the PDG values of the branching fractions are used in the optimization, while the theoretical expectation is used for the B_s^0 search. The optimization is performed separately for the three rare decay modes. The resulting optimal values are very similar between the different modes and the following averages are used for all three searches: $\lambda_{2D}/\sigma(\lambda_{2D}) > 14$, $\Delta\alpha < 0.06$ rad, and $I > 0.6$. The invariant mass distribution for the three searches after applying the optimal requirements on the discriminating variables are shown in Fig. 4.

In the $D\bar{O}$ search, muons are required to have $p_T > 2.5$ GeV and kaon with $p_T > 0.4$ GeV. The $D\bar{O}$ search for the $B_s^0 \rightarrow \phi \mu^+ \mu^-$ decay is op-

timized using the following three discriminating variables: 2D pointing angle $\Delta\alpha$, B candidate isolation I , and the 2D decay length significance $L_{2D}/\sigma(L_{2D})$. $D\bar{O}$ uses a random-grid search to find the optimal values of the discriminants by maximizing the figure-of-merit $\epsilon_S/(a/2 + \sqrt{B})$. The parameter ϵ_S is the efficiency for reconstructing the signal and the constant a is set to 2.0, corresponding to testing the signal hypothesis at the 95% C.L. The number of background events is estimated by extrapolating the high and low-mass sidebands to the signal window. The optimization procedure yields the following values for the discriminating variables: $\Delta\alpha < 0.1$ rad, $I > 0.72$, and $L_{2D}/\sigma(L_{2D}) > 10.3$. The invariant mass distribution after applying optimized selection requirements is shown in Fig. 5.

The branching fraction can be computed by normalizing the number of the observed signal to the number of reconstructed resonant $B \rightarrow hJ/\psi$ decays:

$$\frac{\mathcal{B}(B \rightarrow h\mu^+\mu^-)}{\mathcal{B}(B \rightarrow hJ/\psi)} = \frac{N_{h\mu^+\mu^-}}{N_{hJ/\psi}} \cdot \frac{\epsilon_{hJ/\psi}}{\epsilon_{h\mu^+\mu^-}}. \quad (3)$$

where h is K^+ , K^{*0} , or ϕ . The parameter $N_{h\mu^+\mu^-}$ is either the number of observed signal events or in the case of setting a limit, the upper limit on the number of signal decays, and $N_{hJ/\psi}$ is the number of reconstructed $B \rightarrow hJ/\psi$ events. The efficiency terms $\epsilon_{hJ/\psi}$ and $\epsilon_{h\mu^+\mu^-}$ are the efficiency for reconstructing the normalization and

Experiment Mode	CDF $B^+ \rightarrow \mu^+ \mu^- K^+$	CDF $B_d^0 \rightarrow \mu^+ \mu^- K^{*0}$	CDF $B_s^0 \rightarrow \mu^+ \mu^- \phi$	DØ $B_s^0 \rightarrow \mu^+ \mu^- \phi$
Signal Yield	90	35	11	0
Expected BKG	45.3 ± 5.8	16.5 ± 3.6	3.5 ± 1.5	1.6 ± 0.4
Gaussian significance	4.5	2.9	2.4	—
Rel $\mathcal{B} \times 10^{-3}$	$0.59 \pm 0.15 \pm 0.03$	$0.62 \pm 0.23 \pm 0.07$	$1.24 \pm 0.60 \pm 0.15$	—
Abs $\mathcal{B} \times 10^{-6}$	$0.60 \pm 0.15 \pm 0.04$	$0.82 \pm 0.31 \pm 0.10$	$1.16 \pm 0.56 \pm 0.42$	—
Rel \mathcal{B} 95%CL limit $\times 10^{-3}$	—	—	2.61	7.4
Rel \mathcal{B} 90%CL limit $\times 10^{-3}$	—	—	2.30	5.6

Table 1

Summary of the $B \rightarrow h\mu^+\mu^-$ searches at CDF and DØ. The branching fraction limits are computed using Bayesian method.

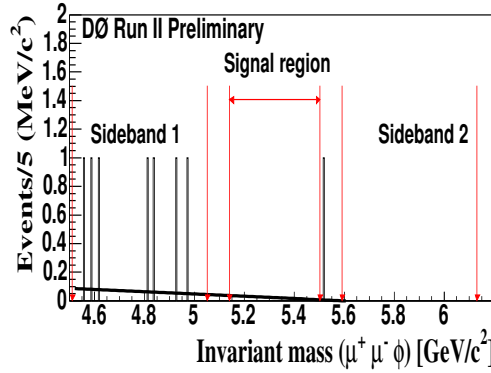


Figure 5. The invariant distribution for the $B_s^0 \rightarrow \phi\mu^+\mu^-$ mode. The solid line shows the sidebands background interpolation into the signal region.

signal decays, respectively.

The branching fraction results and limits are tabulated in Tab. 1. CDF has seen strong evidence of the rare decays in the B^+ and B^0 channels. Neither CDF nor DØ observed significant signal in the B_s^0 channel.

5. CONCLUSIONS

With a subset of currently available dataset, CDF and DØ have made important progress in rare decay searches. The current limit of $B_s^0 \rightarrow \mu^+\mu^-$ is already significantly constraining some scenarios of new physics beyond the SM. In addition, CDF has seen significant evidence of signal in the $B^+ \rightarrow K^+\mu^+\mu^-$ and $B^0 \rightarrow K^{*0}\mu^+\mu^-$ modes. So far, no signal is observed in the $B_s^0 \rightarrow \phi\mu^+\mu^-$ channel. However, the Tevatron

is reaching the SM level of sensitivity; an observation of this mode is expected in the near term.

REFERENCES

1. G. Buchalla and A. J. Buras, Nucl. Phys. **B400**, 225 (1993); A.J. Buras, Phys. Lett. B **566**, 115 (2003).
2. S. Choudhury and N. Gaur, Phys. Lett. B **451**, 86 (1999); K.S. Babu and C. Kolda, Phys. Rev. Lett. **84**, 228 (2000).
3. R. Dermisek *et al.*, J. High Energy Phys. **04**, 037 (2003); D. Auto *et al.*, J. High Energy Phys. **06**, 023 (2003).
4. H. Baer *et al.*, J. High Energy Phys. **07**, 050 (2002); S. Baek, P. Ko, and W.Y. Song, Phys. Rev. Lett. **89**, 271801 (2002); H. Logan and U. Nierste, Phys. Lett. B **566**, 115 (2003); A. Dedes and B. Huffman, Phys. Lett. B **600**, 261 (2004).
5. P. Colangelo, F. De Fazio, R. Ferrandes and T. N. Pham, Phys. Rev. D **73**, 115006 (2006); F. Kruger and J. Matias, Phys. Rev. D **71**, 094009 (2005); T. M. Aliev, A. Ozpineci and M. Savci, Eur. Phys. J. C **29**, 265 (2003).
6. B. Aubert *et al.*, BABAR Collaboration, Phys. Rev. D **73**, 092001 (2006).
7. A. Ishikawa *et al.*, BELLE Collaboration, Phys. Rev. Lett. **96**, 251801 (2006).
8. D. Acosta *et al.*, CDF Collaboration, Phys. Rev. D **71**, 032001 (2005).
9. V. M. Abazov *et al.*, DØ Collaboration, arXiv:physics/0507191.